Protein Labeling

International Edition: DOI: 10.1002/anie.201506935
German Edition: DOI: 10.1002/ange.201506935

Redesign of a Fluorogenic Labeling System To Improve Surface Charge, Brightness, and Binding Kinetics for Imaging the Functional Localization of Bromodomains

*Yuichiro Hori, Shinya Hirayama, Motoki Sato, and Kazuya Kikuchi**

Abstract: *Protein labeling with fluorogenic probes is a powerful method for the imaging of cellular proteins. The labeling time and fluorescence contrast of the fluorogenic probes are critical factors for the precise spatiotemporal imaging of protein dynamics in living cells. To address these issues, we took mutational and chemical approaches to increase the labeling kinetics and fluorescence intensity of fluorogenic PYP-tag probes. Because of charge-reversal mutations in PYP-tag and probe redesign, the labeling reaction was accelerated by a factor of 18 in vitro, and intracellular proteins were detected with an incubation period of only 1 min. The brightness of the probe both in vitro and in living cells was enhanced by the mutant tag. Furthermore, we applied this system to the imaging analysis of bromodomains. The labeled mutant tag successfully detected the localization of bromodomains to acetylhistone and the disruption of the bromodomain–acetylhistone interaction by a bromodomain inhibitor.*

Chemical methods for protein labeling have emerged as an alternative to fluorescent proteins and are attracting attention in the field of bioimaging.[1,2] Some of these new techniques use a protein tag paired with a synthetic fluorescent probe for the specific labeling of intracellular proteins.[1] In particular, fluorogenic probes for the labeling of protein tags are useful tools for live-cell imaging of proteins.[3–14] Whereas free forms of these probes are nonfluorescent, their fluorescence intensity increases following labeling reactions. Because of this beneficial property, the location of proteins in living cells can be quickly verified without the necessity for washout procedures to remove free probes. Following a report on the probe FlAsH and its tag,[3] various fluorogenic probes were developed for the labeling of intracellular proteins fused to protein tags, such as the SNAP-tag,[4–6] the HaloTag,[6] the BL-tag,[7] the TMP-tag,[8] FAPs,[9] the dC10α-tag,[10] and the photoactive yellow protein tag (PYP-tag).[11] Key factors for the performance of fluorogenic systems are labeling time and fluorescence contrast. In current "no-wash" systems, labeling reactions are conducted with an incubation time of more than 10 min to provide fluorescence images of intracellular proteins with sufficient contrast,[5–10,12] with the exception of the PYP-tag paired with its probe, which rapidly detects cellular proteins in 6 min.[11] However, even these time periods are long enough for the removal of free probes by washing cells. Thus, further efforts to acquire fluorescence images with shorter incubation times are required for making the best use of fluorogenic systems. The fine-tuning of a protein tag and its probe is essential to fulfill this requirement and will lead to practical biological applications, which have been limited thus far.

We have developed a PYP-tag-based labeling system.[11,13] The small size of PYP-tag (14 kDa) makes it attractive for use as a protein tag. Previously, we designed and synthesized the fluorogenic probes TMBDMA and CMBDMA for intracellular protein labeling.[11] These probes contain a newly designed PYP-tag ligand, which is an environment-sensitive fluorophore. Fluorescence enhancement is triggered by recruiting these probes to a hydrophobic ligand-binding pocket in PYP-tag, whereas the probe loses fluorescence in a high-polarity aqueous buffer. Of these two probes, CMBDMA shows more interesting properties. Despite its anionic net charge, the probe can cross cell membranes. Furthermore, we noticed that live-cell images obtained with CMBDMA are brighter than those obtained with TMBDMA (see Figure S1 in the Supporting Information). Thus, CMBDMA is more practical and suitable for the high-contrast live-cell imaging of proteins. However, CMBDMA requires more than 10 min for the intracellular imaging of PYP-tagged proteins. Therefore, the labeling reactions need to be accelerated for rapid imaging and to take advantage of the fluorogenic probe. In this study, to solve this problem, we created a PYP-tag mutant, in which the charges on the protein surface were modulated, and redesigned the chemical structure of CMBDMA (Figure 1a). Furthermore, the labeling system was applied to bromodomain imaging. Bromodomain is an epigenetic reader-protein domain that binds to acetylhistone and plays an important role in transcriptional activation.[15] Small molecules that inhibit the bromodomain–acetylhistone interaction are expected to be promising drugs for the treatment of cancer and inflammation.[15] Thus, the development of a live-cell assay for examining this interaction is in high demand. In this study, by using our redesigned labeling system, we conducted live-cell analyses of the bromodomain–acetylhistone interaction.

Previous results suggested that the charges of PYP-tag contribute to its labeling kinetics.[11] To investigate the effects

[*] Dr. Y. Hori, S. Hirayama, M. Sato, Prof. K. Kikuchi
Graduate School of Engineering, Osaka University
Osaka 565-0871 (Japan)
E-mail: kkikuchi@mls.eng.osaka-u.ac.jp
Dr. Y. Hori, Prof. K. Kikuchi
IFReC, Osaka University
Osaka 565-0871 (Japan)
Dr. Y. Hori
JST, PRESTO
Osaka 565-0871 (Japan)

Supporting information for this article is available on the WWW under http://dx.doi.org/10.1002/anie.201506935.

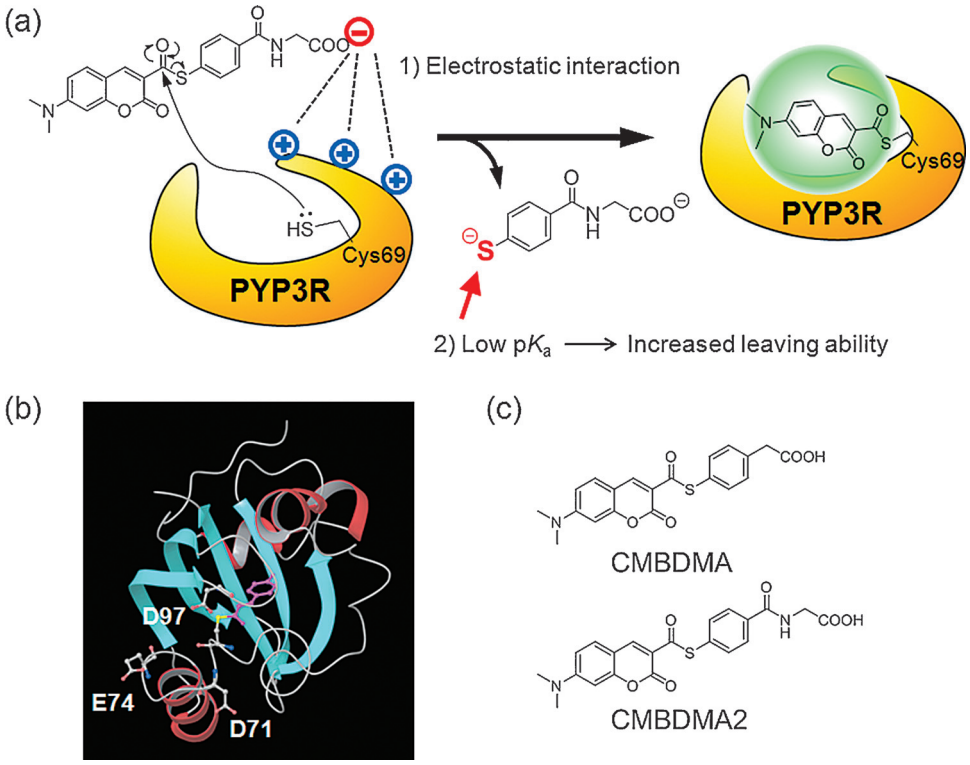

Figure 1. a) Design of the PYP-tag mutant PYP3R and its fluorogenic probe, with a focus on electrostatic interactions and the pK_a value of the leaving group. b) Structure of PYP (PDB ID: 1otb). A natural PYP-tag ligand is indicated in magenta. c) Chemical structures of CMBDMA and CMBDMA2.

of surface charges close to the ligand-binding pocket on labeling reactions, we analyzed three mutants, PYP-D71R, PYP-E74R, and PYP-D97R, in which each anionic residue was converted into arginine (Figure 1b). All the mutants bound covalently to CMBDMA and enhanced the fluorescence intensity (see Figures S2a and S3 and Table S1 in the Supporting Information). The mutants reacted with CMBDMA more rapidly than the wild-type PYP-tag (PYPwt; see Table S2 and Figure S4). These results indicate that electrostatic interaction between the probe and PYP-tag enhances labeling reactions. Interestingly, as compared with PYPwt, PYP-D71R enhanced the fluorescence of CMBDMA more intensely at an excitation wavelength of 450 nm (see Figure S3). It is known that dialkylaminocoumarins emit strong fluorescence from the intramolecular-charge-transfer (ICT) state.[16] One probable reason for the higher fluorescence enhancement is that the mutation affects the protein conformation around the fluorophore and leads to the promotion of emission from the ICT state. However, further structural analysis will be required to verify the detailed mechanism.

Next, we created a novel mutant with three arginine residues at these amino acid positions, PYP3R (Figure 1a), with the expectation that the triple mutation would further enhance both the brightness and the labeling kinetics of CMBDMA. In labeling reactions of PYP3R, the fluorescence intensity increased notably, and was 62% higher than that of the probe bound to PYPwt (see Figures S2a and S3). The labeling reaction of PYP3R was faster than that of PYPwt (see Table S2 and Figure S4). The k_2 value of PYP3R with CMBDMA was determined to be $1.3\times10^3\,M^{-1}s^{-1}$, whereas PYPwt binds to the probe with a k_2 value of $1.1\times10^2\,M^{-1}s^{-1}$. These results indicate that the triple mutation significantly improved brightness and labeling kinetics.

To further improve labeling kinetics, we redesigned the probe structure by scrutinizing the labeling mechanism. When CMBDMA binds to PYP-tag through transthioesterification with Cys69, a thiophenyl moiety is released from the probe. A previous study suggested that the pK_a value of the leaving group of CMBDMA could affect the labeling kinetics.[11] Thus, we developed a new probe, CMBDMA2, which has a thiophenyl leaving group with a lower pK_a value (Figure 1a,c; see also Scheme S1 in the Supporting Information). The thiophenyl group has the electron-drawing carbonyl group of an amide at the *para* position and is estimated to have a pK_a value of 5.8, whereas the pK_a value of the corresponding thiol of CMBDMA is estimated to be 6.9.[17,18] CMBDMA2 covalently labeled both PYPwt and PYP3R (see Figure S2b), and increased fluorescence intensity (see Figure S5). A model structure of the labeled PYP3R was created by using MacroModel (see Figure S6). The background hydrolysis reaction of CMBDMA2 was not detected (see Figure S7). Specific labeling in cell lysate was observed (see Figure S2c). CMBDMA2 bound to PYPwt with a k_2 value of $6.2\times10^2\,M^{-1}s^{-1}$, which is 5.6 times higher than that of CMBDMA (see Table S2 and Figure S4). Furthermore, the combinatorial use of PYP3R and CMBDMA2 led to a remarkable acceleration of the labeling kinetics ($k_2=2.0\times10^3\,M^{-1}s^{-1}$) by a factor of 18 in comparison with the labeling kinetics of the parent pair, PYPwt and CMBDMA. These results clearly indicate that the lowering of the pK_a value of the leaving group promoted labeling reactions.

No-wash live-cell imaging of intracellular proteins was conducted by adding CMBDMA2 to HEK293T cells transfected with the fusion gene of maltose binding protein (MBP) with PYPwt (MBP-PYPwt) or PYP3R (MBP-PYP3R). Fluorescence was observed only from CMBDMA2-treated cells expressing these genes (see Figure S8a). Cells transfected with the genes of PYP-tags fused to nuclear localization signals (PYPwt-NLS and PYP3R-NLS) were also imaged by using CMBDMA2. The cells exhibited fluorescence from their nuclei, but only when the cells expressed the

PYP constructs (see Figure S8b). These results show that CMBDMA2 permeated the cell membrane, specifically labeled intracellular proteins, and enabled the imaging of protein localization. Moreover, PYP3R and CMBDMA2 gave brighter fluorescence than the pair composed of PYPwt and CMBDMA when the same measurement conditions were used (see Figure S1). Importantly, the CMBDMA2/PYP3R-NLS pair enabled the rapid and clear detection of fluorescence in nuclei only 1 min after the addition of the probe (Figure 2). The fluorescence signal was saturated after 3 min,

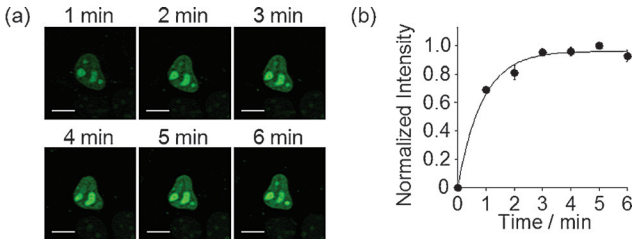

Figure 2. Time-lapse imaging with CMBDMA2. a) Fluorescence images of PYP3R-NLS acquired after the addition of CMBDMA2 (5 μM). The excitation wavelength was 473 nm. Scale bar: 5 μm. b) Time course of fluorescence intensity, as quantified by the use of imaging data for CMBDMA2-treated cells expressing PYP3R-NLS ($N = 5$).

whereas the pair composed of CMBDMA and PYPwt required more than 20 min for the saturation of fluorescence intensity (see Figure S8c,d).

Finally, we conducted live-cell imaging of bromodomains. We fused the PYP-tags with bromodomains of BRD4[19] (PYPwt-BRD or PYP3R-BRD). In PYPwt-BRD-expressing cells, fluorescence was observed throughout nuclei (Figure 3a). In contrast, the fluorescence in PYP3R-BRD-expressing cells was observed to be uneven. Quantitative analysis confirmed that as compared to PYPwt-BRD, PYP3R-BRD was distributed less homogeneously (Figure 3b,c). This difference might be explained by considering the p*I* values of the PYP-tags. Whereas PYPwt is an acidic protein with a calculated p*I* value of 4.8, PYP3R has a p*I* value of 6.7.[20] The anionic properties of PYPwt may cause a decrease in affinity for nucleosomes containing acetylhistone owing to electrostatic repulsion of DNA. Thus, it is possible that PYPwt-BRD may be partially dissociated from the nucleosome, thus causing a more uniform distribution of fluorescence, whereas PYP3R-BRD might be localized to genomic regions rich in acetylhistone, since the repulsive interaction between the protein tag and DNA is diminished, thus causing a nonuniform distribution of fluorescence. A previous report also showed that endogenous BRD4 was localized in a speckled pattern similar to that of PYP3R-BRD, thus suggesting that the tagging of PYPwt affected the localization of BRD4.[21]

To check the localization of the bromodomains to acetylhistone, we used a bromodomain inhibitor, JQ-1, which binds to bromodomains and interrupts bromodomain–acetylhistone interactions.[19] We found that the fluorescence derived from PYP3R-BRD was distributed more uniformly in the presence of JQ1 (Figure 3a). This observation is supported by quantitative analysis (Figure 3b,c). These results strongly suggest that PYP3R-BRD is localized to acetylhistone-containing nucleosomes, and that JQ1 causes dissociation of the fusion protein from the acetylhistone. Importantly, this system is useful for investigating the effect of bromodomain inhibitors in live cells. Previously, GFP, which is also an acidic protein, was fused to BRD4 and was used to analyze the inhibition of the bromodomain–acetylhistone interaction.[19,22] However, fluorescence recovery after photobleaching (FRAP) was applied to examine inhibitory effects of bromodomain inhibitors. In these studies, no clear change of the fluorescence localization was observed in the presence of inhibitors. In contrast, the surface-charge mutations of PYP-tag led to a clear change in the localization of bromodomains in the presence of a bromodomain inhibitor.

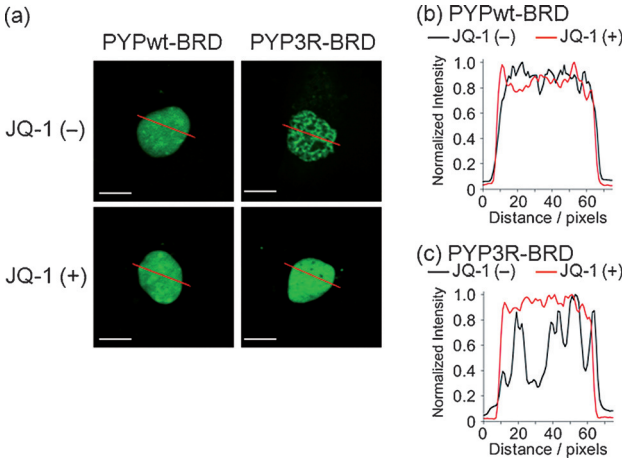

Figure 3. Imaging of the bromodomain–acetylhistone interaction and its inhibition. a) Fluorescence images of CMBDMA2-treated NIH3T3 cells expressing PYPwt-BRD and PYP3R-BRD in the absence or presence of JQ-1. The excitation wavelength was 473 nm. The probe (5 μM) was incubated with the cells for 5 min. Scale bar: 10 μm. b,c) Fluorescence profiles plotted along the red lines in (a).

In summary, we redesigned a PYP-tag–fluorogenic-probe pair by using mutational and chemical approaches that focused on electrostatic interaction and pK_a values. The new tag–probe pair rapidly detected fluorescence signals of proteins inside living cells after a significantly shorter incubation time (1 min) than that reported previously and showed greater brightness than that of a previous pair composed of PYPwt and CMBDMA. These features and the small size of the tag are attractive advantages for protein labeling. Furthermore, this system was successfully applied to the detection of bromodomain–acetylhistone interactions. Previously, inhibition of the bromodomain–acetylhistone interaction was only detected in living cells by the use of special microscopic techniques, such as FRAP. Furthermore, our results suggest that the mutational modulation of protein surface charges provides a useful and promising strategy for live-cell imaging with protein-tag systems. The redesigned labeling system is valuable as an easy-to-use analytical tool to examine the bromodomain interaction and its inhibition. We believe that this new tool will also be useful for various live-cell studies on the localization, movement, and interaction of proteins.

Acknowledgements

This research was supported by JST, PRESTO, by MEXT of Japan (Grants 25220207, 26102529, 15K12754 to K.K., 26282215 to Y.H. and 26.755 to S.H.), by CREST of JST, by the Asahi Glass Foundation, by the Uehara Memorial Foundation, by the Naito Foundation, by the Mochida Memorial Foundation for Medical and Pharmaceutical Research, and by the Program for Creating Future Wisdom, Osaka University, selected in 2014.

Keywords: bromodomains · fluorescent probes · fluorogenic systems · protein labeling · protein modifications

How to cite: *Angew. Chem. Int. Ed.* **2015**, *54*, 14368–14371
Angew. Chem. **2015**, *127*, 14576–14579

[1] S. Mizukami, Y. Hori, K. Kikuchi, *Acc. Chem. Res.* **2014**, *47*, 247–256.
[2] C. P. Ramil, Q. Lin, *Chem. Commun.* **2013**, *49*, 11007–11022.
[3] B. A. Griffin, S. R. Adams, R. Y. Tsien, *Science* **1998**, *281*, 269–272.
[4] X. Sun, A. Zhang, B. Baker, L. Sun, A. Howard, J. Buswell, D. Maurel, A. Masharina, K. Johnsson, C. J. Noren, M. Q. Xu, I. R. Correa, Jr., *ChemBioChem* **2011**, *12*, 2217–2226.
[5] a) T. K. Liu, P. Y. Hsieh, Y. D. Zhuang, C. Y. Hsia, C. L. Huang, H. P. Lai, H. S. Lin, I. C. Chen, H. Y. Hsu, K. T. Tan, *ACS Chem. Biol.* **2014**, *9*, 2359–2365; b) T. Komatsu, K. Johnsson, H. Okuno, H. Bito, T. Inoue, T. Nagano, Y. Urano, *J. Am. Chem. Soc.* **2011**, *133*, 6745–6751.
[6] a) J. B. Grimm, B. P. English, J. Chen, J. P. Slaughter, Z. Zhang, A. Revyakin, R. Patel, J. J. Macklin, D. Normanno, R. H. Singer, T. Lionnet, L. D. Lavis, *Nat. Methods* **2015**, *12*, 244–250; b) G. Lukinavicius, K. Umezawa, N. Olivier, A. Honigmann, G. Yang, T. Plass, V. Mueller, L. Reymond, I. R. Correa, Jr., Z. G. Luo, C. Schultz, E. A. Lemke, P. Heppenstall, C. Eggeling, S. Manley, K. Johnsson, *Nat. Chem.* **2013**, *5*, 132–139.
[7] S. Mizukami, S. Watanabe, Y. Akimoto, K. Kikuchi, *J. Am. Chem. Soc.* **2012**, *134*, 1623–1629.
[8] C. Jing, V. W. Cornish, *ACS Chem. Biol.* **2013**, *8*, 1704–1712.
[9] S. L. Schwartz, O. Yan, C. A. Telmer, K. A. Lidke, M. P. Bruchez, D. S. Lidke, *Acs Chem. Biol.* **2015**, *10*, 539–546.
[10] Y. Chen, C. M. Clouthier, K. Tsao, M. Strmiskova, H. Lachance, J. W. Keillor, *Angew. Chem. Int. Ed.* **2014**, *53*, 13785–13788; *Angew. Chem.* **2014**, *126*, 14005–14008.
[11] Y. Hori, T. Norinobu, M. Sato, K. Arita, M. Shirakawa, K. Kikuchi, *J. Am. Chem. Soc.* **2013**, *135*, 12360–12365.
[12] R. Borra, D. Dong, A. Y. Elnagar, G. A. Woldemariam, J. A. Camarero, *J. Am. Chem. Soc.* **2012**, *134*, 6344–6353.
[13] a) Y. Hori, H. Ueno, S. Mizukami, K. Kikuchi, *J. Am. Chem. Soc.* **2009**, *131*, 16610; b) Y. Hori, K. Nakaki, M. Sato, S. Mizukami, K. Kikuchi, *Angew. Chem. Int. Ed.* **2012**, *51*, 5611–5614; *Angew. Chem.* **2012**, *124*, 5709–5712.
[14] Y. Hori, K. Kikuchi, *Curr. Opin. Chem. Biol.* **2013**, *17*, 644–650.
[15] P. Filippakopoulos, S. Knapp, *Nat. Rev. Drug Discovery* **2014**, *13*, 337–356.
[16] S. Nad, M. Kumbhakar, H. Pal, *J. Phys. Chem. A* **2003**, *107*, 4808–4816.
[17] The pK_a value was calculated by using the Epik program (Schrödinger K.K.).
[18] J. C. Shelley, A. Cholleti, L. L. Frye, J. R. Greenwood, M. R. Timlin, M. Uchimaya, *J. Comput.-Aided Mol. Des.* **2007**, *21*, 681–691.
[19] P. Filippakopoulos, J. Qi, S. Picaud, Y. Shen, W. B. Smith, O. Fedorov, E. M. Morse, T. Keates, T. T. Hickman, I. Felletar, M. Philpott, S. Munro, M. R. McKeown, Y. Wang, A. L. Christie, N. West, M. J. Cameron, B. Schwartz, T. D. Heightman, N. La Thangue, C. A. French, O. Wiest, A. L. Kung, S. Knapp, J. E. Bradner, *Nature* **2010**, *468*, 1067–1073.
[20] The p*I* values were calculated by using ExPASy COMPUTE pI/MW (http://web.expasy.org/compute_pi/).
[21] M. K. Jang, K. Mochizuki, M. Zhou, H. S. Jeong, J. N. Brady, K. Ozato, *Mol. Cell* **2005**, *19*, 523–534.
[22] S. Picaud, D. Da Costa, A. Thanasopoulou, P. Filippakopoulos, P. V. Fish, M. Philpott, O. Fedorov, P. Brennan, M. E. Bunnage, D. R. Owen, J. E. Bradner, P. Taniere, B. O'Sullivan, S. Müller, J. Schwaller, T. Stankovic, S. Knapp, *Cancer Res.* **2013**, *73*, 3336–3346.

Received: July 27, 2015
Published online: October 5, 2015

